FULL PAPER

Dalton
www.rsc.org/dalton

Tertiary phosphine binding to pyridylazole chelated rhenium *via* substitution in phosphine oxide precursors: geometrical preference, twin isomerization and effects of diphosphine spacer length and metal oxidation state

Suman Sengupta,[a] Jaydip Gangopadhyay[a] and Animesh Chakravorty *[a,b]

[a] *Department of Inorganic Chemistry, Indian Association for the Cultivation of Science, Kolkata, 700 032, India. E-mail: icac@mahendra.iacs.res.in*

[b] *Jawaharlal Nehru Centre for Advanced Scientific Research, Bangalore, 560 064, India*

Received 9th July 2003, Accepted 19th September 2003
First published as an Advance Article on the web 13th October 2003

The bimolecular reaction of $[Re^{V}L(O)Cl_3]$ [L = 2-(2-pyridyl)benzoxazole (L^1), 2-(2-pyridyl)benzthiazole (L^2)], **1** with excess diphosphine $[Ph_2P(CH_2)_xPPh_2$ (x = 1–4)] has furnished $[Re^{III}L(OP(Ph)_2(CH_2)_xP(Ph)_2)Cl_3]$, **2** which is spontaneously converted in solution to $[Re^{III}L(P(Ph)_2(CH_2)_xP(O)(Ph)_2)Cl_3]$, **4**. The reaction of $[Re^{III}L(OPMe_yPh_{3-y})Cl_3]$, **3** with PMe_yPh_{3-y} (y = 0–2) has afforded $[Re^{III}L(PMe_yPh_{3-y})Cl_3]$, **5**. Oxidation of **2** and **3** by dilute nitric acid has furnished nitrates of the rhenium(IV) species, $\mathbf{2}^+$ and $\mathbf{3}^+$. Structure determination *vis-à-vis* spectral and electrochemical comparisons have revealed a meridional geometry for **2**, **3**, $\mathbf{2}^+$, and $\mathbf{3}^+$ and a facial geometry for **4** and **5**. The transformation **2** ⟶ **4** is a twin isomerization (linkage-cum-geometrical), the geometrical part of which recurs in the conversion **3** ⟶ **5**. Rate studies have revealed that the reaction **2** ⟶ **4** is intramolecular in nature. It is initiated by nucleophilic attack of the metal by the dangling phosphine function. The process slows down nearly exponentially as the diphosphine spacer length (x) increases. The oxidised complex $\mathbf{2}^+$ does not isomerize.

Introduction

This work has originated from our interest in oxygen atom transfer reactions between monooxorhenium(V) reagents and tertiary phosphines.[1–7] The available results primarily concern monophosphines. Diphosphines are potentially interesting but have attracted only limited attention so far.[8–10] Recently we reported a pair of oxo chelates of type $[Re^{V}L(O)Cl_3]$, **1**, where L is 2-(2-pyridyl)benzoxazole (L^1) or 2-(2-pyridyl)benzthiazole (L^2).

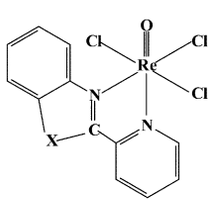

X = O, $[ReL^1(O)Cl_3]$
X = S, $[ReL^2(O)Cl_3]$

1

These underwent facile bimolecular oxygen atom transfer reactions with the monophosphines (PR_3, R = Me/Ph) furnishing the corresponding phosphine oxide complexes as shown schematically in eqn. (1).[11]

$$Re^{V}{\equiv}O + PR_3 \longrightarrow Re^{III}{-}OPR_3 \qquad (1)$$

The present work was initiated to scrutinise the transfer reactions of **1** with a group of linear diphosphines bearing a polymethylene spacer of variable length. Attention has been focussed on the transfer of one oxygen atom only so that phosphine oxide complexes with a dangling phosphine function are generated. The latter function could be a potential nucleophile that might attack the metal site within the same molecule. Such reactivity has indeed been observed providing an opportunity to scrutinise the effects of diphosphine spacer length and metal oxidation state. To model the observed phenomenon monophosphorus species of type $Re^{III}(OPR_3)$, $Re^{IV}(OPR_3)$ and $Re^{III}(PR_3)$ have also been examined. The complexes have been characterised with the help of spectral, electrochemical and crystallographic data. The factors controlling structure and reactivity are scrutinised.

Results and discussion

Compound types and their synthesis

Four diphosphines and three monophosphines have been employed in the present work: $Ph_2P(CH_2)_xPPh_2$ (x = 1–4) and PMe_yPh_{3-y} (y = 0–2). All the complexes reported below have been isolated in excellent yields. In order to achieve transfer of only one oxygen atom to the diphosphines, excess of the latter was reacted (eqn. (2))

$$\mathbf{1} + Ph_2P(CH_2)_xPPh_2 \longrightarrow \mathbf{2} \qquad (2)$$

with **1** in dichloromethane solution furnishing the species of type **2** where D is coordinated at oxygen. The monophosphorus complexes of type **3** except y = 2 are known.[11]

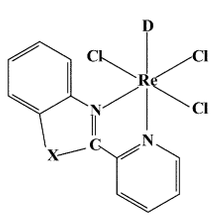

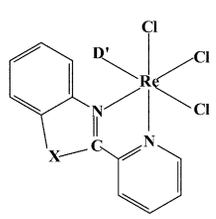

2, D = $OP(Ph)_2(CH_2)_XP(Ph)_2$
3, D = $OPMe_yPh_{3-y}$

4, D' = $P(Ph)_2(CH_2)_XP(O)(Ph)_2$
5, D' = PMe_yPh_{3-y}

The rate of the reaction of eqn. (2) has been determined spectrophotometrically in dichloromethane solution at 308 K for the x = 4 case where the subsequent isomerization (*vide infra*) proceeds very slowly. In the presence of excess diphosphine the rate of transfer is proportional to the concentration

DOI: 10.1039/b307834e

Table 1 Rate constants for the reaction of $[ReL(O)Cl_3]$ with $[Ph_2P(CH_2)_4PPh_2]$ in dichloromethane solution at 308 K[a]

L	$10^2[Ph_2P(CH_2)_4PPh_2]$/M	10^2k_{obs}/min^{-1}	k/M^{-1} min^{-1}
L[1]	1.06	1.65(0.01)	1.84(0.01)
	1.40	2.29(0.01)	
	2.00	3.38(0.01)	
L[2]	1.06	0.77(0.01)	0.85(0.01)
	1.40	1.07(0.01)	
	2.00	1.57(0.01)	

[a] The initial concentration of $[ReL(O)Cl_3]$ is 1.25×10^{-4} M. Least-squares deviations are given in parentheses.

of **1** and the observed rate constant is proportional to the concentration of phosphine implying a second order rate law. The k values (Table 1) which lie close to those for the reaction of $[ReL(O)Cl_3]$ with $PMePh_2$ follow the order $[ReL^1(O)Cl_3] > [ReL^2(O)Cl_3]$ as expected.[11]

The complexes of type **2** are inherently reactive in dichloromethane solution, the dangling phosphine function displacing the coordinated phosphine oxide function furnishing **4** where D′ is coordinated at phosphorus. This linkage isomerization is simultaneously attended by meridional ⟶ facial geometrical isomerization. The nature and rate of this twin isomerization process will be examined later. The geometrical part in the **2** ⟶ **4** transformation has been realised in monophosphorus species. Thus upon treating the meridional phosphine oxide complexes of type **3** with excess PMe_yPh_{3-y} in boiling benzene facial phosphine complexes of type **5** are formed, eqn. (3).

$$\mathbf{3} + PMe_yPh_{3-y} \longrightarrow \mathbf{5} + OPMe_yPh_{3-y} \qquad (3)$$

The phosphine oxide complexes **2** and **3** underwent facile metal oxidation upon treatment with dilute nitric acid in acetonitrile solution furnishing the corresponding rhenium(IV) cations $\mathbf{2}^+$ and $\mathbf{3}^+$ which were isolated as nitrates in the representative cases of $[Re^{IV}L(OP(Ph)_2CH_2P(Ph)_2)Cl_3]^+$ and $[Re^{IV}L(OPPh_3)Cl_3]^+$. The nitrates act as 1 : 1 electrolytes in methanol solution (Λ, 92–99 Ω^{-1} cm^2 mol^{-1}). Attempted oxidation of the phosphine complexes **4** and **5** by dilute nitric acid furnished highly insoluble compounds which could not be characterised.

Spectra and electrochemistry

In the visible region (400–900 nm) **2**–**5** display multiple transitions of moderate intensity (ε, 1000–5000 dm^3 mol^{-1} cm^{-1}) in the form of peaks and shoulders. The most prominent feature occurs around 740 nm in **2** and **3** and around 700 nm in **4** and **5**. An idealised $t_{2g}(Re) \longrightarrow \pi^*(L)$ MLCT assignment is consistent with the observed shift to higher energy in going from phosphine oxide (**2**, **3**) to phosphine coordination (**4**, **5**) which stabilises the t_{2g} shell *via* back-bonding. This is also reflected in the significant increase of the Re^{IV}/Re^{III} reduction potentials (*vide infra*). The rhenium(IV) species $\mathbf{2}^+$ and $\mathbf{3}^+$ in which MLCT transitions are expected to shift to much higher energies, do not display any band in the visible region except for a weak shoulder around 430 nm.

Two or three Re–Cl stretches occur in all the complexes (300–350 cm^{-1}) along with a C=N stretch near 1600 cm^{-1}. The coordinated P–O stretch (**2**, **3**) is observed near 1130 cm^{-1} as compared to ≈ 1180 cm^{-1} characterising uncoordinated P–O (**4**). In $\mathbf{2}^+$ and $\mathbf{3}^+$ the oxidised metal weakens the P–O bond and the vibration frequency drops to ≈ 1115 cm^{-1}. The ν_3 vibration[12] of NO_3^- is seen at 1384 cm^{-1} in the nitrates of $\mathbf{2}^+$ and $\mathbf{3}^+$.

All the complexes display paramagnetically shifted[2,3,8,11,13,14] ^{1}H NMR spectra which have characteristic chemical shifts for each type of compound. Well-resolved spin–spin structures are seen for **2**–**5** but not for $\mathbf{2}^+$ and $\mathbf{3}^+$. The L proton resonances occur in the ranges 5 to 30 ppm (**2**, **3**), −12 to 25 ppm (**4**, **5**) and 4 to 57 ppm ($\mathbf{2}^+$, $\mathbf{3}^+$). The aromatic protons of the phosphorus ligands resonate in the range 4 to 9 ppm (**2**, **3**), 5 to 20 ppm (**4**, **5**) and 5 to 10 ppm ($\mathbf{2}^+$, $\mathbf{3}^+$). Lastly, the CH_2/Me resonances fall in the ranges −11 to −1 ppm (**2**, **3**), −4 to 8 ppm (**4**, **5**) and 4 to 7 ppm ($\mathbf{2}^+$, $\mathbf{3}^+$).

Table 2 Selected bond distances (Å) and angles (°) for compound **3a**

Re–N1	2.054(6)	Re–Cl2	2.361(3)
Re–N2	2.063(6)	Re–Cl3	2.367(2)
Re–O	2.078(5)	P–O	1.520(6)
Re–Cl1	2.402(2)		
N1–Re–N2	77.5(3)	N1–Re–O	172.7(3)
N2–Re–O	95.3(2)	N1–Re–Cl2	89.8(2)
N2–Re–Cl2	90.0(2)	O–Re–Cl2	89.5(2)
N1–Re–Cl3	91.4(2)	N2–Re–Cl3	90.8(2)
O–Re–Cl3	89.4(2)	Cl2–Re–Cl3	178.71(8)
N1–Re–Cl1	96.2(2)	N2–Re–Cl1	173.6(2)
O–Re–Cl1	91.0(2)	Cl2–Re–Cl1	88.81(8)
Cl3–Re–Cl1	90.49(8)	P–O–Re	140.1(4)

The complexes uniformly display a nearly reversible Re^{IV}/Re^{III} couple, in acetonitrile solution, the cyclic voltammetric peak-to-peak separation being 60–80 mV. The reduction potentials lie near 0.24 V *vs.* SCE in **2** and **3**[11] and near 0.58 V in **4** and **5**. The sizeable difference of reduction potentials makes it possible to observe the isomerization of **2** to **4** electrochemically as shown in Fig. 1. Quantitative isomerization studies are however best made spectrophotometrically, *vide infra*. The voltammograms of $\mathbf{2}^+$ and $\mathbf{3}^+$ (initial scan cathodic) are virtually superimposable on those of the corresponding **2** and **3** species (initial scan anodic). The t_{2g} shell in **4** and **5** is stabilised by back-bonding to phosphorus (*vide infra*) and an increase of the reduction potential is indeed expected in going from phosphine oxide to phosphine coordination.

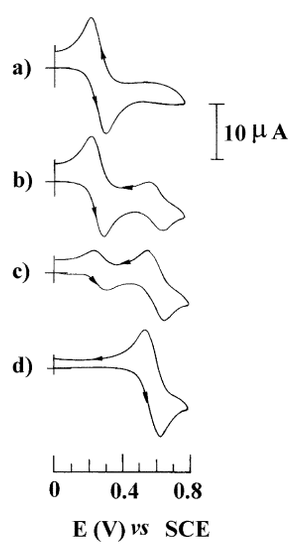

Fig. 1 Cyclic voltammetric observation of the isomerization of $[ReL^2(OP(Ph)_2CH_2P(Ph)_2)Cl_3]$ in acetonitrile solution in the time domain 0–24 h : (a) 0 h, (b) 2 h, (c) 6 h, (d) 24 h.

Structures

The structures of $[ReL^2(OPMe_2Ph)Cl_3]$, **3a**; $[ReL^2(OPPh_3)Cl_3]NO_3 \cdot 0.5CH_2Cl_2$, $\mathbf{3b}^+NO_3^- \cdot 0.5CH_2Cl_2$; $[ReL^1(PMe_2Ph)Cl_3]$, **5a** and $[ReL^1(PMePh_2)Cl_3] \cdot H_2O$, $\mathbf{5b} \cdot H_2O$ have been determined. Perspective views are shown in Fig. 2–5 and selected bond parameters are listed in Tables 2, 3 and 4.

The type **3** complexes reported earlier did not afford single crystals suitable for determination of a satisfactorily refined structure.[11] This has now been achieved with the new complex **3a**. The severely distorted octahedral geometry has a meridional disposition of chloride ligands (Fig. 2). The pyridine ring makes a dihedral angle of 16.9° with the benzthiazole moiety and consequently the ReL^2 fragment is not quite planar (mean

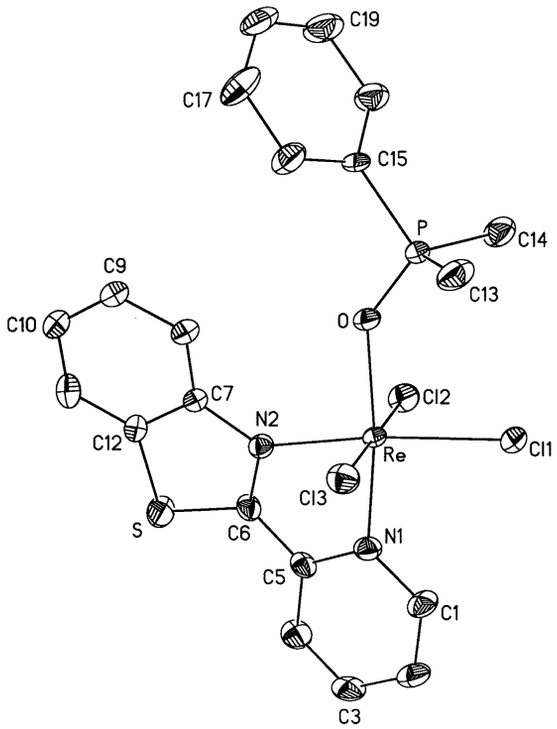

Fig. 2 A perspective view of $[ReL^2(OPMe_2Ph)Cl_3]$ **3a**. The atoms are represented by their 30% thermal probability ellipsoids.

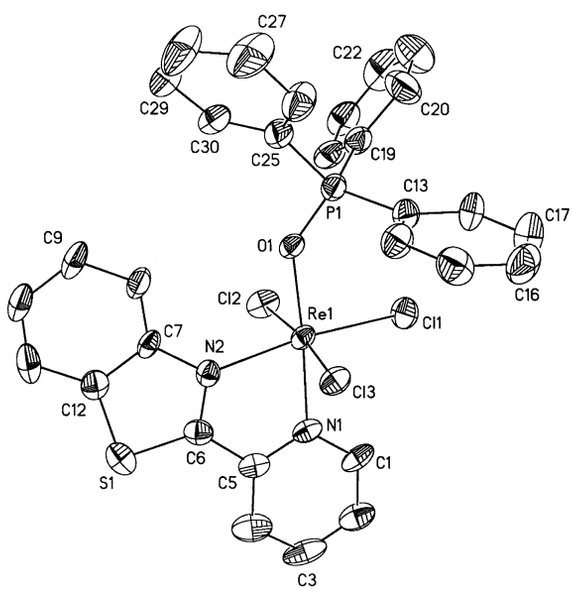

Fig. 3 A perspective view of molecule 1 of $[ReL^2(OPPh_3)Cl_3]^+$ $\mathbf{3b}^+$. The atoms are represented by their 30% thermal probability ellipsoids.

deviation 0.18 Å). The P atom lies 2.65 and 2.73 Å away from the centroids of the octahedral faces defined by O, Cl(1), Cl(3) and O, Cl(1), Cl(2) respectively. The corresponding distances from the centroids of the O, N(2), Cl(2) and O, N(2), Cl(3) faces are > 3.1Å. The nucleophilic attack of PMe_2Ph on $[ReL^2(O)Cl_3]$ had logically occurred near the less hindered faces defined by the chloride and oxo ligands.

The asymmetric unit of $\mathbf{3b}^+NO_3^-\cdot 0.5CH_2Cl_2$ consists of two structurally very similar but crystallographically distinct $\mathbf{3b}^+$ cations (along with two nitrate ions and one dichloromethane molecule), only one of the cations being shown in Fig. 3. The geometry of the $\mathbf{3b}^+$ cation is grossly similar to that of **3a** but the ReL^2 fragment is more planar (average mean deviation 0.05 Å) in this case. The metal–ligand bond lengths of $\mathbf{3b}^+$ are significantly different from those of **3a**. The average Re–Cl

Table 3 Selected bond distances (Å) and angles (°) for compound $\mathbf{3b}^+NO_3^-\cdot 0.5CH_2Cl_2$

Molecule 1		Molecule 2	
Re–N1	2.115(8)	Re51–N51	2.122(8)
Re–N2	2.113(8)	Re51–N52	2.134(8)
Re–O1	2.034(6)	Re51–O51	2.002(6)
Re1–Cl1	2.298(3)	Re51–Cl51	2.292(3)
Re1–Cl2	2.336(3)	Re51–Cl52	2.323(3)
Re1–Cl3	2.304(3)	Re51–Cl53	2.317(3)
P1–O1	1.532(7)	P51–O51	1.529(7)
N1–Re1–N2	76.7(4)	N51–Re51–N52	77.5(3)
N2–Re1–O1	99.0(3)	N52–Re51–O51	97.4(3)
N2–Re1–Cl2	84.7(2)	N52–Re51–Cl52	85.4(2)
N1–Re1–Cl3	87.9(2)	N51–Re51–Cl53	88.0(2)
O1–Re1–Cl3	90.6(2)	O51–Re51–Cl53	89.8(2)
N1–Re1–C11	93.7(3)	N51–Re51–Cl51	92.8(3)
O1–Re1–C11	90.6(2)	O51–Re51–Cl51	92.5(2)
Cl3–Re1–Cl1	94.39(13)	Cl53–Re51–Cl51	93.59(12)
N1–Re1–O1	175.5(3)	N51–Re51–O51	174.4(3)
N1–Re1–Cl2	89.6(2)	N51–Re51–Cl52	91.2(2)
O1–Re1–Cl2	91.3(2)	O51–Re51–Cl52	90.5(2)
N2–Re1–Cl3	88.7(2)	N52–Re51–Cl53	88.9(2)
Cl2–Re1–Cl3	173.38(11)	Cl52–Re51–Cl53	174.28(10)
N2–Re1–C11	169.8(3)	N52–Re51–Cl51	169.8(2)
Cl2–Re1–C11	91.90(13)	Cl52–Re51–Cl51	92.10(12)
P1–O1–Re1	140.4(4)	P51–O51–Re51	159.4(5)

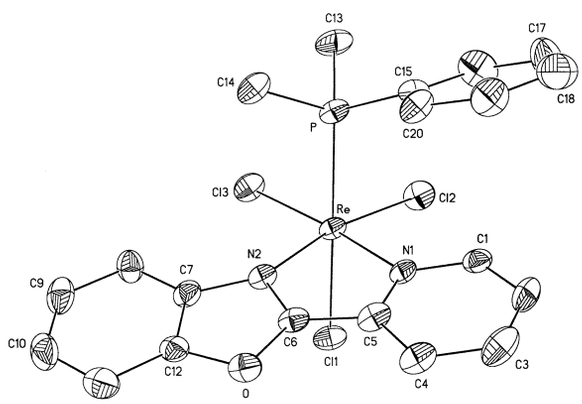

Fig. 4 A perspective view of $[ReL^1(PMe_2Ph)Cl_3]$ **5a**. The atoms are represented by their 30% thermal probability ellipsoids.

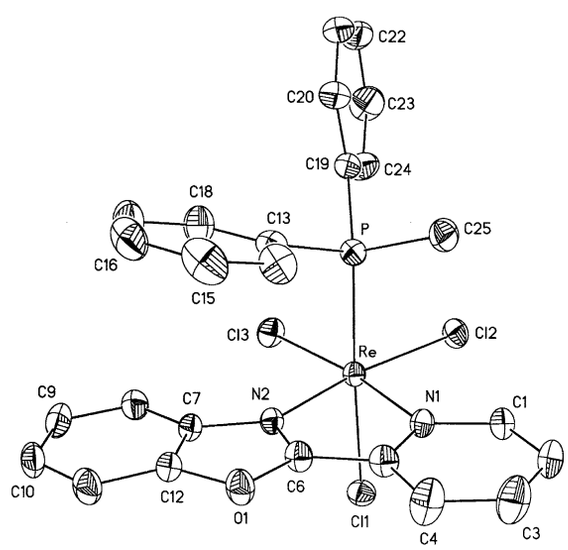

Fig. 5 A perspective view of $[ReL^1(PMePh_2)Cl_3]$ **5b**. The atoms are represented by their 30% thermal probability ellipsoids.

and Re–O distances in $\mathbf{3b}^+$ are respectively ≈ 0.07 and ≈ 0.06 Å shorter than those in **3a**. These bonds are primarily σ in character and the contraction of metal radius upon oxidation is

Table 4 Selected bond distances (Å) and angles (°) for compounds **5a** and **5b**·H_2O

	5a	**5b**·H_2O
Re–N1	2.089(8)	2.110(5)
Re–N2	2.060(8)	2.098(5)
Re–Cl1	2.408(3)	2.438(2)
Re–Cl2	2.338(3)	2.354(2)
Re–Cl3	2.349(3)	2.358(2)
Re–P	2.373(3)	2.414(2)
N2–Re–N1	76.4(3)	75.7(2)
N1–Re–Cl2	93.6(2)	93.66(13)
N1–Re–Cl3	171.3(2)	170.76(13)
N2–Re–P	96.5(2)	91.23(14)
Cl2–Re–P	89.17(11)	88.25(6)
N2–Re–Cl1	84.1(2)	88.69(14)
Cl2–Re–Cl1	90.39(11)	91.13(6)
P–Re–Cl1	178.73(9)	176.18(5)
N2–Re–Cl2	168.6(2)	169.40(13)
N2–Re–Cl3	95.2(2)	95.02(13)
Cl2–Re–Cl3	94.97(11)	95.58(6)
N1–Re–P	91.7(2)	88.89(13)
Cl3–Re–P	86.86(10)	91.73(6)
N1–Re–Cl1	89.5(2)	87.38(13)
Cl3–Re–Cl1	91.99(10)	92.09(6)

registered in their lengths. In striking contrast, the average Re–N distance in $\mathbf{3b}^+$ is ≈ 0.07 Å longer than that in **3a**. Trivalent rhenium is a potent π-donor[3,8,16] but metal oxidation is expected to diminish the donor power very considerably. The longer Re–N bond in $\mathbf{3b}^+$ is believed to reflect the weakness or absence of back-bonding in the $Re^{IV}L^2$ fragment.

In both **5a** and **5b** the $ReCl_3$ fragment is facially disposed (Fig. 4 and 5), the L^1 ligand is approximately planar and so is the ReL^1 fragment. The average Re–Cl distances are virtually the same as that in **3a** (2.37–2.38 Å). On the other hand, the average Re–N length of **5a** and **5b** is ≈ 0.03 Å longer. This is consistent with the presence of Re–P back-bonding which diminishes the demand on π*(L) orbitals as compared to that in **3a** where only Re–L^2 back-bonding is possible (phosphine oxide is a pure σ-donor). In the lattice of **5b**·H_2O there are actually two types of water molecule: one lying in a general position but displaying a two-fold disorder with respect to a crystallographic C_2 axis and the other sitting on a special position (two-fold axis). The two water molecules of adjacent symmetry related complexes are strongly hydrogen bonded (2.531(7) Å).

When phosphine and L are coligands, the net back-bonding is stronger in the facial (as opposed to meridional) arrangement in which the competition between the two ligands for identical metal orbitals is minimal. Thus **5** has facial geometry while **3** (here only L is π acidic) assumes the sterically and electrostatically superior meridional configuration. The strong geometrical differences between $Re(PR_3)Cl_3$ and $Re(OPR_3)Cl_3$ chelates of π-acidic N,N donor ligands appear to be a general phenomenon which has previously been documented by us in the cases of pyridylaldimine[13] and azo[2,8,9] ligands.

Phosphine bulk inequality (cone angle, $PMe_2Ph < PMePh_2$) has a subtle effect on metal–ligand bond lengths (**5a < 5b**). The difference in the case of the Re–P bond is ≈0.04 Å. The type **5** compounds with the bulkier PPh_3 did not afford suitable crystals but the average Re–P distances in related facial complexes[8,13] bearing PPh_3 coordination is ≈0.07 Å longer than that in **5b**.

The diphosphorus compounds of types **2**, **4** and $\mathbf{2}^+$ did not afford suitable single crystals for structure determination. However, on the basis of spectral and electrochemical analogy with the monophosphorus species it is clear that these have the same gross structures as **3**, **5** and $\mathbf{3}^+$ respectively.

Table 5 Rate constants for the isomerization of $[ReL(OP(Ph)_2(CH_2)_x P(Ph)_2)Cl_3]$ in dichloromethane solution at 308 K[a]

L	*x*	10^4[$ReL(OP(Ph)_2(CH_2)_xP(Ph)_2)Cl_3$]/M	10^3k/min^{-1}
L^1	1	1.25	5.05(0.03)
		2.50	5.07(0.02)
		3.75	5.06(0.03)
	2	1.25	2.44(0.01)
	3	1.25	0.95(0.01)
	4	1.25	0.40(0.01)
L^2	1	1.25	2.17(0.01)
		2.50	2.16(0.01)
		3.75	2.17(0.01)
	2	1.25	1.08(0.01)
	3	1.25	0.43(0.01)
	4	1.25	0.15(0.01)

[a] Least-squares deviations are given in the parentheses.

Twin isomerization

The spontaneous isomerization of **2** to **4** (eqn. (4)),

$$\mathbf{2} \longrightarrow \mathbf{4} \qquad (4)$$

has been examined spectrophotometrically at 308 K in dichloromethane solution. Time evolution spectra are characterised by multiple isosbestic points in the visible region (Fig. 6). The rate of the reaction is independent of the concentration of **2** consistent with its intramolecular nature. The rate constants for the family of type **2** species are collected in Table 5.

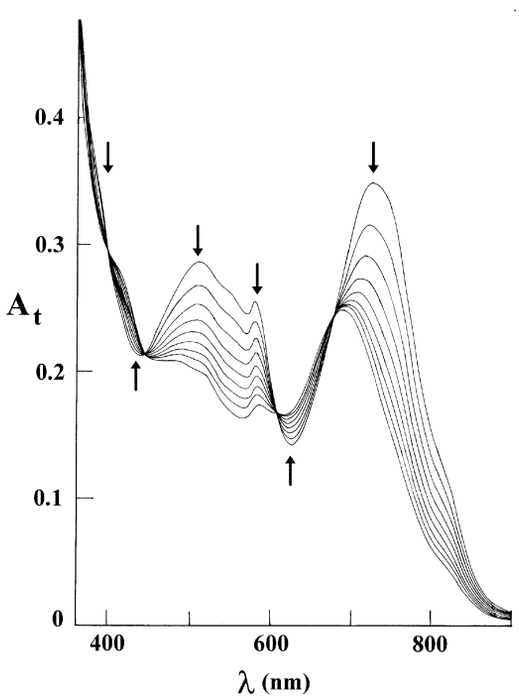

Fig. 6 Time evolution spectra for the twin isomerization reaction of $[ReL^1(OP(Ph)_2CH_2P(Ph)_2)Cl_3]$ in dichloromethane solution at 308 K (A_t is absorbance).

It is logical to assume that the transformation is initiated *via* nucleophilic attack of the metal by the dangling phosphine function. The isomerization rates of the L^1 complexes are systematically higher (nearly twice) than those of the corresponding L^2 species. This is consistent with heteroatom electronegativity (O > S) which makes the metal more susceptible to attack in the L^1 complexes. The attack is stylised in Scheme 1 where a less crowded OCl_2 face near which the phosphine oxide ligand is likely to be positioned (see structure of **3a**) is shown to be the site of initial action. The transformation can then

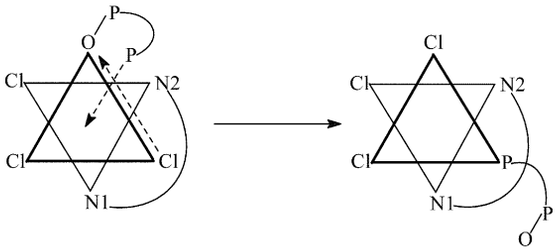

Scheme 1

progress rationally *via* edge displacement[8,17] of a chloride ligand resulting in the relay substitutions: Re–OP by Re–Cl and of Re–Cl by Re–P. The net effect is twin isomerization (Scheme 1). An alternative pathway involving direct transfer of oxygen from phosphorus to phosphorus is energetically highly unlikely since it requires the synchronous dissociation of both P–O and Re–O bonds.

The rate of the isomerization reaction of eqn. (4) decreases rapidly as the spacer length increases. The dependence on x is exponential (Fig. 7) to a good degree. The number of possible conformations of the dangling $(CH_2)_xPPh_2$ fragment is indeed expected to increase exponentially as x increases,[15] but only a few of the conformations will be spatially suited (proximal metal and phosphine site) for the reaction to occur. We have previously observed twin isomerizations similar to those reported here in two cases of azoheterocyclic complexes where the process took place exclusively in the $x = 1$ case.[8,9] The eight compounds reported here have provided the first opportunity to observe the isomerization process in the domain of x spanning 1–4.

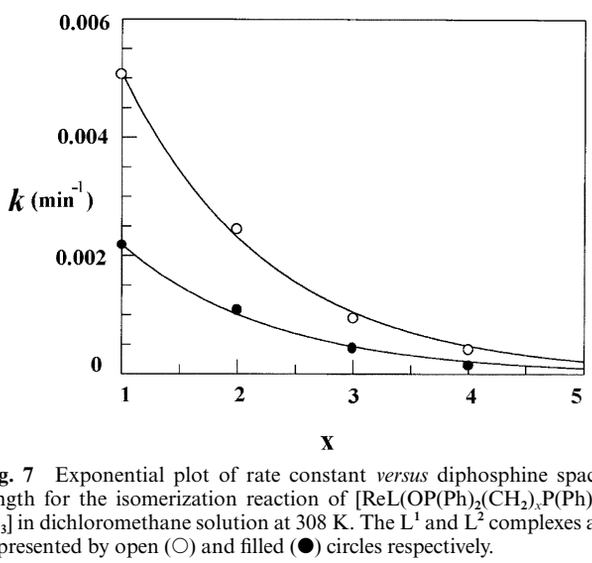

Fig. 7 Exponential plot of rate constant *versus* diphosphine spacer length for the isomerization reaction of $[ReL(OP(Ph)_2(CH_2)_xP(Ph)_2)Cl_3]$ in dichloromethane solution at 308 K. The L^1 and L^2 complexes are represented by open (○) and filled (●) circles respectively.

Upon oxidation of the metal to the tetravalent state as in $\mathbf{2}^+$, the isomerization process is completely arrested even when $x = 1$ which corresponds to maximum reactivity in the case of **2**. Coulometric reduction of $\mathbf{2}^+$ to **2** reestablishes the isomerization process. The lack of reactivity of $\mathbf{2}^+$ could be a reflection of the kinetic inertness of the d^3 configuration in rhenium(IV). Other factors are also expected to work in the same direction. Thus rhenium(IV) is a harder acceptor than rhenium(III) and oxygen is a harder donor than phosphorus. This as well as the weaker back-bonding ability of rhenium(IV) as revealed by the structural data is expected to disfavour the attack of the metal by the dangling phosphine function. On these grounds $[Re^{IV}L(OPPh_3)Cl_3]^+$ should also be unreactive towards substitution by PPh_3. However, the conditions required for converting **3** to **5** (eqn. (3)) are relatively drastic (excess phosphine, boiling benzene) and under these conditions the tetravalent complex is spontaneously reduced to $[Re^{III}L(OPPh_3)Cl_3]$ which then reacts as in eqn. (3).

Conclusion

It is demonstrated that the family **2** formed from $[ReL(O)Cl_3]$ and $Ph_2P(CH_2)_xPPh_2$ (x = 1–4) undergoes spontaneous intramolecular linkage-cum-geometrical isomerization in solution affording **4**. The same geometrical isomerization recurs in the conversion of **3** to **5**.

Significant $Re^{III}L$ (**2**–**5**) and $Re^{III}P$ (**4**, **5**) back-bonding characterises the species and this logically plays a crucial role in directing the course of isomerization and in determining the trend (**4**(**5**) > **2**(**3**)) of MLCT excitation energy and Re^{IV}/Re^{III} reduction potential.

The rate of the reaction **2** ⟶ **4** falls rapidly with increasing x as expected from the statistics of polymethylene conformation. The isomerization halts completely upon metal oxidation as in $\mathbf{2}^+$. Ongoing studies include scrutiny of the activation parameters of the **2** ⟶ **4** reaction and the search for other families that display spacer regulated twin isomerization.

Experimental

The $[ReL(O)Cl_3]$ complexes were prepared as before.[11] HPLC grade acetonitrile was used for electrochemical work and all other chemicals and solvents were of reagent grade and were used as received. Spectral measurements were carried out using the following equipment: UV-vis, Shimadzu UV 1601 PC spectrophotometer fitted with thermostated cell compartments (sh is shoulder); IR (KBr disc), Perkin-Elmer L-0100 and Nicolet Magna IR 750 Series II spectrometers; ^{1}H NMR, Bruker 300 MHz spectrometer (s, singlet; d, doublet; t, triplet; i, ill-resolved and m, multiplet). A Perkin-Elmer 2400 Series II elemental analyzer was used for microanalysis (C, H, N). Solution electrical conductivity was measured in methanol with a Phillips PR 9500 bridge using a platinized electrode (cell constant of 1.05). Electrochemical measurements were performed under a nitrogen atmosphere using a CHI model 620A electrochemical analyzer, with a platinum working electrode. The supporting electrolyte was tetraethylammonium perchlorate (TEAP), and the potentials are referenced to the saturated calomel electrode (SCE) without junction correction.

Synthesis of complexes

$[ReL(OP(Ph)_2(CH_2)_xP(Ph)_2)Cl_3]$ 2. These were prepared by a general procedure: reaction of $[ReL(O)Cl_3]$ with excess $Ph_2P(CH_2)_xPPh_2$ in dichloromethane solution. Details are given below for a representative case.

$[ReL^1(OP(Ph)_2CH_2P(Ph)_2)Cl_3]$. To a solution of $[ReL^1(O)Cl_3]$ (65 mg, 0.13 mmol) in 10 cm^3 dichloromethane was added 150 mg (0.39 mmol) of $Ph_2PCH_2PPh_2$. The resulting solution was magnetically stirred for 3.5 h at room temperature, and during this time the colour changed from yellow to violet. The solution was then subjected to chromatography on a silica gel column (25 × 1 cm, 60–120 mesh). Excess diphosphine was eluted with benzene. The violet band that followed was eluted with a benzene–acetonitrile (25 : 1) mixture. Solvent removal from the eluate under reduced pressure afforded $[ReL^1(OP(Ph)_2CH_2P(Ph)_2)Cl_3]$ as a violet solid. Yield: 68% (Found: C, 50.08; H, 3.49; N, 3.08. Calc. for $C_{37}H_{30}N_2O_2P_2Cl_3Re$: C, 49.98; H, 3.40; N, 3.15%). UV-vis [λ_{max}/nm (ε/dm^3 mol^{-1} cm^{-1}), CH_2Cl_2 solution]: 812^{sh} (1090), 730 (2850), 580 (2060), 547^{sh} (2110), 510 (2310), 389^{sh} (2710), 305 (27870). IR(cm^{-1}): 300, 309, 332 (Re–Cl), 1127 (O–P), 1593 (C=N). ^{1}H NMR [δ (J/Hz), $CDCl_3$ solution]: L^1, 21.90 (d, J = 7.5, 1H), 10.90 (d, J = 7.8, 1H), 10.54 (t, J = 7.8, 1H), 10.23 (d, J = 6.3, 1H), 8.97 (t, J = 8.6, 1H), 8.19 (t, J = 7.2, 1H), 6.80 (t, J = 7.5, 1H), 6.17 (d, J = 7.8, 1H); $Ph_2PCH_2PPh_2$, −9.77 (s, 2H, CH_2), 7.86 (m, 2H), 7.56 (m, 2H), 7.36 (m, 2H), 7.19 (m, 2H), 6.77 (m, 2H), 6.64 (t, J = 7.5, 2H), 6.29 (m, 4H), 4.66 (t, J = 7.7, 2H), 4.36 (t, J = 8.0, 2H).

$[ReL^2(OP(Ph)_2CH_2P(Ph)_2)Cl_3]$. Yield: 70% (Found: C, 49.00; H, 3.31; N, 3.02. Calc. for $C_{37}H_{30}N_2OP_2SCl_3Re$: C, 49.09;

H, 3.34; N, 3.09%). UV-vis [λ_{max}/nm (ε/dm^3 mol^{-1} cm^{-1}), CH_2Cl_2 solution]: 815^{sh} (2260), 739 (4480), 585 (3190), 517 (3000), 475^{sh} (2760), 398^{sh} (3510), 328 (19610). IR(cm^{-1}) : 305, 330 (Re–Cl), 1135 (O–P), 1591 (C=N). ^{1}H NMR [δ (*J*/Hz), $CDCl_3$ solution]: L^2, 28.95 (d, *J* = 7.8, 1H), 22.54 (d, *J* = 6.2, 1H), 22.15 (t, *J* = 6.5, 1H), 11.05 (d, *J* = 8.1, 1H), 10.72 (t, *J* = 7.5, 1H), 8.31 (t, *J* = 7.5, 1H), 7.78 (t, *J* = 7.5, 1H), 6.59 (d, *J* = 7.3, 1H); $Ph_2PCH_2PPh_2$, −10.70 (s, 2H, CH_2), 8.42 (t, *J* = 8.7, 4H), 8.08 (t, *J* = 7.4, 6H), 7.18 (m, 2H), 6.59 (t, *J* = 6.8, 2H), 6.42 (m, 2H), 6.34 (t, *J* = 7.5, 4H).

[ReL^1(OP(Ph)$_2$(CH$_2$)$_2$P(Ph)$_2$)Cl$_3$]. Yield: 69% (Found: C, 50.66; H, 3.50; N, 3.18. Calc. for $C_{38}H_{32}N_2O_2P_2Cl_3Re$: C, 50.53; H, 3.57; N, 3.10%). UV-vis [λ_{max}/nm (ε/dm^3 mol^{-1} cm^{-1}), CH_2Cl_2 solution]: 810^{sh} (1110), 732 (2810), 578 (1870), 547^{sh} (2000), 508 (2170), 386^{sh} (2380), 306 (26950). IR(cm^{-1}) : 310, 328 (Re–Cl), 1131 (O–P), 1593 (C=N). ^{1}H NMR [δ (*J*/Hz), $CDCl_3$ solution]: L^1, 27.57 (d, *J* = 6.1, 1H), 21.36 (d, *J* = 7.5, 1H), 11.05 (t, *J* = 7.7,1H), 10.45 (t, *J* = 7.5, 1H), 8.74 (t, *J* = 8.4, 1H), 8.07 (d, *J* = 6.1, 1H), 6.55 (d, *J* = 6.2, 1H), 5.83 (t, *J* = 6.4, 1H); $Ph_2P(CH_2)_2PPh_2$, −1.20 (m, 2H, CH_2), −2.84 (m, 2H, CH_2), 8.83 (i, 2H), 8.38 (d, *J* = 7.8, 2H), 7.89 (m, 4H), 7.68 (d, *J* = 6.1, 2H), 7.48 (m, 4H), 7.03 (t, *J* = 7.5, 2H), 6.89 (t, *J* = 7.3, 2H), 5.68 (t, *J* = 7.2, 2H).

[ReL^2(OP(Ph)$_2$(CH$_2$)$_2$P(Ph)$_2$)Cl$_3$]. Yield: 72% (Found: C, 49.72; H, 3.44; N, 2.95. Calc. for $C_{38}H_{32}N_2OP_2SCl_3Re$: C, 49.65; H, 3.51; N, 3.05%). UV-vis (λ_{max}/nm (ε/dm^3 mol^{-1} cm^{-1}), CH_2Cl_2 solution]: 813^{sh} (2080), 738 (4340), 584 (3040), 516 (2930), 475^{sh} (2700), 396^{sh} (3450), 328 (18530). IR(cm^{-1}: 301, 308, 329 (Re–Cl), 1136 (O–P), 1593 (C=N). ^{1}H NMR [δ (*J* /Hz),$CDCl_3$ solution]: L^2, 23.83 (d, *J* = 8.1, 1H), 23.18 (t, *J* = 6.3, 1H) 23.05 (d, *J* = 6.1, 1H), 11.52 (d, *J* = 8.1, 1H), 10.77 (t, *J* = 7.7, 1H), 9.12 (i,1H), 7.64 (t, *J* = 7.2, 1H), 7.04 (t, *J* = 7.7, 1H); $Ph_2P(CH_2)_2PPh_2$, −2.45 (m, 2H, CH_2), −2.77 (m, 2H, CH_2), 9.12 (m, 2H), 8.27 (t, *J* = 7.2, 2H), 8.06 (d, *J* = 7.4, 4H), 7.94 (t, *J* = 7.5, 4H), 7.36 (i, 2H), 6.91 (t, *J* = 7.4, 2H), 5.69 (t, *J* = 7.1, 2H), 5.24 (m, 2H).

[ReL^1(OP(Ph)$_2$(CH$_2$)$_3$P(Ph)$_2$)Cl$_3$]. Yield: 71% (Found: C, 51.16; H, 3.66; N, 3.11. Calc. for $C_{39}H_{34}O_2N_2P_2Cl_3Re$: C, 51.07; H, 3.74; N, 3.05%). UV-vis (λ_{max}/nm (ε/dm^3 mol^{-1} cm^{-1}), CH_2Cl_2 solution]: 812^{sh} (1180), 734 (2800), 579 (1960), 546^{sh} (2090), 514 (2230), 387^{sh} (2520), 305 (26520). IR(cm^{-1}): 302, 310, 331 (Re–Cl), 1128 (O–P), 1590 (C=N). ^{1}H NMR [δ (*J*/Hz), $CDCl_3$ solution]: L^1, 25.51 (d, *J* = 7.8, 1H), 21.72 (d, *J* = 7.8, 1H), 10.89 (t, *J* = 7.7, 1H), 10.53 (t, *J* = 7.7, 1H), 8.81 (i, 1H), 7.90 (t, *J* = 7.7, 1H), 6.63 (t, *J* = 7.9, 1H), 6.28 (d, *J* = 8.0, 1H); $Ph_2P(CH_2)_3PPh_2$, −1.86 (m, 2H, CH_2), −3.11 (m, 2H, CH_2), −4.14 (m, 2H, CH_2), 8.53 (t, *J* = 7.8, 2H), 8.08 (t, *J* = 7.2, 2H), 7.80 (m, 2H), 7.55 (t, *J* = 7.1, 2H), 7.2–7.3 (m, 4H), 6.89 (t, *J* = 7.5, 2H), 6.51 (t, *J* = 6.7, 2H), 6.34 (t, *J* = 7.5, 2H), 6.08 (t, *J* = 8.6, 2H).

[ReL^2(OP(Ph)$_2$(CH$_2$)$_3$P(Ph)$_2$)Cl$_3$]. Yield: 73% (Found: C, 50.29; H, 3.60; N, 2.90. Calc. for $C_{39}H_{34}N_2OP_2SCl_3Re$: C, 50.19; H, 3.67; N, 3.00%). UV-vis (λ_{max}/nm (ε/dm^3 mol^{-1} cm^{-1}), CH_2Cl_2 solution]: 812^{sh} (2290), 739 (4420), 585 (3170), 517 (2990), 475^{sh} (2760), 396^{sh} (3460), 328 (18280). IR(cm^{-1}): 304, 332 (Re–Cl), 1125 (O–P), 1603 (C=N). ^{1}H NMR [δ (*J*/Hz), $CDCl_3$ solution]: L^2, 28.20 (d, *J* = 7.8, 1H), 22.62 (t, *J* = 6.2, 1H), 22.33 (d, *J* = 7.3, 1H), 10.97 (d, *J* = 8.3, 1H), 10.39 (t, *J* = 7.7, 1H), 8.22 (t, *J* = 7.5, 1H), 8.01 (t, *J* = 7.5, 1H), 7.93 (d, *J* = 8.2, 1H); $Ph_2P(CH_2)_3PPh_2$, −3.37 (m, 2H, CH_2), −4.46 (m, 2H, CH_2), −6.76 (m, 2H, CH_2), 8.89 (i, 2H), 7.81 (m, 6H), 7.49 (t, *J* = 7.4, 4H), 7.30 (i, 2H), 7.21 (t, *J* = 8.1, 4H), 6.43 (t, *J* = 8.6, 2H).

[ReL^1(OP(Ph)$_2$(CH$_2$)$_4$P(Ph)$_2$)Cl$_3$]. Yield: 73% (Found: C, 51.50; H, 3.82; N, 3.09. Calc. for $C_{40}H_{36}N_2O_2P_2Cl_3Re$: C, 51.59; H, 3.90; N, 3.01%). UV-vis (λ_{max}/nm (ε/dm^3 mol^{-1} cm^{-1}), CH_2Cl_2 solution]: 815^{sh} (1150), 735 (2770), 579 (1930), 547^{sh} (2040), 512 (2170), 384^{sh} (2500), 306 (24500). IR(cm^{-1}): 301, 308, 327 (Re–Cl), 1127 (O–P), 1587 (C=N). ^{1}H NMR [δ (*J*/Hz), $CDCl_3$ solution]: L^1, 21.43 (d, *J* = 7.5, 1H), 21.22 (d, *J* = 7.5, 1H), 17.58 (t, *J* = 6.1, 1H), 10.54 (t, *J* = 6.6, 1H), 8.23 (d, *J* = 8.2, 2H), 7.11 (t, *J* = 8.4, 1H), 5.61 (t, *J* = 7.2, 1H); $Ph_2P(CH_2)_4PPh_2$, −3.87 (m, 2H, CH_2), −4.61 (m, 2H, CH_2), −5.34 (m, 2H, CH_2), −7.69 (m, 2H, CH_2), 8.84 (t, *J* = 8.1, 2H), 8.46 (i, 2H), 8.01 (i, 2H), 7.68 (m, 4H), 6.89 (i, 2H), 6.43 (m, 4H), 5.53 (m, 2H), 3.96 (m, 2H).

[ReL^2(OP(Ph)$_2$(CH$_2$)$_4$P(Ph)$_2$)Cl$_3$]. Yield: 76% (Found: C, 50.67; H, 3.89; N, 3.05. Calc. for $C_{40}H_{36}N_2OP_2SCl_3Re$: C, 50.72; H, 3.83; N, 2.96%). UV-vis (λ_{max}/nm (ε/dm^3 mol^{-1} cm^{-1}), CH_2Cl_2 solution]: 812^{sh} (2220), 740 (4520), 585 (3320), 519 (3080), 475^{sh} (2800), 396^{sh} (3410), 328 (20090). IR(cm^{-1}): 303, 307, 325 (Re–Cl), 1127 (O–P), 1593 (C=N). ^{1}H NMR [δ (*J*/Hz), $CDCl_3$ solution]: L^2, 29.64 (d, *J* = 7.8, 1H), 28.41 (d, *J* = 7.7, 1H), 22.64 (t, *J* = 6.2, 1H), 15.50 (d, *J* = 6.9, 1H), 13.32 (d, *J* = 7.2, 1H), 10.54 (t, *J* = 7.7, 1H), 7.67 (t, *J* = 7.8, 1H), 6.56 (t, *J* = 8.4, 1H); $Ph_2P(CH_2)_4PPh_2$, −4.56 (m, 2H, CH_2), −5.32 (m, 2H, CH_2), −5.75 (m, 2H, CH_2), −6.62 (m, 2H, CH_2), 8.1–8.4 (m, 4H), 7.97 (d, *J* = 7.6, 4H), 7.87 (d, *J* = 7.0, 2H), 7.78 (t, *J* = 7.9, 2H), 7.48 (t, *J* = 8.1, 6H), 6.71 (i, 2H).

[ReL(OPMe$_y$Ph$_{3-y}$)Cl$_3$] 3. The *y* = 0 and 1 complexes are known.[11] The *y* = 2 complexes were prepared similarly in 80% yields.

[ReL^1(OPMe$_2$Ph)Cl$_3$]. (Found: C, 37.42; H, 3.06; N, 4.30. Calc. for $C_{20}H_{19}N_2O_2PCl_3Re$: C, 37.36; H, 2.98; N, 4.36%) UV-vis (λ_{max}/nm (ε/dm^3 mol^{-1} cm^{-1}), CH_2Cl_2 solution]: 813^{sh} (1040), 732 (2680), 576 (1830), 547^{sh} (2090), 503 (2140), 388^{sh} (2650), 319 (12900). IR(cm^{-1}): 310, 331 (Re–Cl), 1130 (O–P), 1600 (C=N). ^{1}H NMR [δ (*J*/Hz), $CDCl_3$ solution]: L^1, 25.47 (d, *J* = 7.8, 1H), 22.92 (d, *J* = 7.8, 1H), 22.23 (t, *J* = 6.5, 1H), 11.07 (t, *J* = 7.4, 1H), 9.65 (d, *J* = 6.3, 1H), 8.39 (t, *J* = 6.9, 1H), 6.17 (t, *J* = 8.1, 1H), 2.36 (d, *J* = 8.1, 1H); PMe_2Ph, −1.49 (s, 3H, PCH_3), −3.19 (s, 3H, PCH_3), 10.80 (t, *J* = 7.8, 2H), 7.86 (t, *J* = 7.7, 1H), 7.14 (d, *J* = 7.8, 2H).

[ReL^2(OPMe$_2$Ph)Cl$_3$]. (Found: C, 36.40; H, 2.98; N, 4.29. Calc. for $C_{20}H_{19}N_2OPSCl_3Re$: C, 36.45; H, 2.91; N, 4.25%) UV-vis (λ_{max}/nm (ε/dm^3 mol^{-1} cm^{-1}), CH_2Cl_2 solution]: 815^{sh} (2480), 742 (4690), 586 (3340), 515 (3140), 475^{sh} (2950), 396^{sh} (3730), 329 (20630). IR(cm^{-1}): 302, 309,327 (Re–Cl), 1131 (O–P), 1593 (C=N). ^{1}H NMR [δ (*J*/Hz), $CDCl_3$ solution]: L^2, 29.68 (d, *J* = 7.8, 1H), 22.79 (t, *J* = 6.3, 1H), 22.21 (d, *J* = 6.4, 1H), 11.32 (t, *J* = 7.7, 1H), 11.16 (d, *J* = 9.0, 1H), 9.3–9.4 (m, 2H), 8.16 (d, *J* = 7.5, 1H); PMe_2Ph, −2.08 (s, 3H, PCH_3), −2.12 (s, 3H, PCH_3), 8.45 (t, *J* = 7.8, 2H), 8.3–8.4 (m, 3H).

[ReL(P(Ph)$_2$(CH$_2$)$_x$P(O)(Ph)$_2$)Cl$_3$] 4. The general procedure consisted of simply leaving a dichloromethane solution of [ReL(OP(Ph)$_2$(CH$_2$)$_x$P(Ph)$_2$)Cl$_3$] to isomerize at room temperature (≈298 K) in a stoppered flask for 1, 2, 4 and 5 days (L = L^1) and 2, 3, 5 and 7 days (L = L^2) for the cases of *x* = 1, 2, 3 and 4 respectively. Procedural details are given below for a representative case.

[ReL^1(P(Ph)$_2$CH$_2$P(O)(Ph)$_2$)Cl$_3$]. A 75 mg (0.08 mmol) sample of [ReL^1(OP(Ph)$_2$CH$_2$P(Ph)$_2$)Cl$_3$] was dissolved in 25 cm^3 of dichloromethane, and the solution was left for 24 h. It was then subjected to chromatography on a silica gel column. A green band was eluted with a benzene–acetonitrile (25 : 10) mixture. Solvent removal under reduced pressure afforded [ReL^1(P(Ph)$_2$CH$_2$P(O)(Ph)$_2$)Cl$_3$] as a green solid which was dried under vacuum over fused $CaCl_2$. Yield: 91% (Found: C, 49.90; H, 3.48; N, 3.28. Calc. for $C_{37}H_{30}N_2O_2P_2Cl_3Re$: C, 49.98; H, 3.40; N, 3.15%). UV-vis [λ_{max}/nm (ε/dm^3 mol^{-1} cm^{-1}), CH_2Cl_2 solution]: 679 (1730), 516 (820), 484^{sh} (900), 445 (1180), 414 (1730), 317 (8130). IR(cm^{-1}): 312, 320 (Re–Cl), 1195 (P–O), 1592 (C=N). ^{1}H NMR [δ (*J*/Hz), $CDCl_3$ solution]: L^1, 18.82 (t, *J* = 6.3, 1H), 17.59 (d, *J* = 8.1, 1H), 16.44 (d, *J* = 6.5, 1H), 8.37 (t, *J* = 7.5, 1H), 6.07 (d, *J* = 7.8, 1H), 5.47 (t, *J* = 7.8, 1H), 0.86 (d, *J* = 7.8, 1H), −3.81 (t, *J* = 8.2, 1H); $(Ph)_2PCH_2P(O)(Ph)_2$, −2.85 (m, 2H, CH_2), 19.53 (d, *J* = 7.2, 2H), 18.63 (d, *J* = 7.3, 2H), 10.33 (t, *J* = 7.1, 2H), 10.09 (t, *J* = 7.7, 2H), 9.43 (t, *J* = 6.9,

2H), 8.91 (t, J = 7.8, 2H), 8.17 (m, 2H), 7.62 (t, J = 7.2, 2H), 7.48 (m, 2H), 6.95 (t, J = 6.8, 2H).

[ReL²(P(Ph)₂CH₂P(O)(Ph)₂)Cl₃]. Yield: 85% (Found: C, 49.02; H, 3.27; N, 3.03. Calc for $C_{37}H_{30}N_2OP_2SCl_3Re$: C, 49.09; H, 3.34; N, 3.09%). UV-vis [λ_{max}/nm (ε/dm³ mol⁻¹ cm⁻¹), CH_2Cl_2 solution]: 707 (3240), 513 (1490), 460^{sh} (1940), 419 (3220), 323 (13660). IR(cm⁻¹): 311, 322 (Re–Cl), 1179 (P–O), 1591 (C=N). ^{1}H NMR [δ (J/Hz), $CDCl_3$ solution]: L², 18.60 (d, J = 6.9, 1H), 17.87 (d, J = 7.2, 1H), 12.62 (d, J = 6.2, 1H), 9.51 (t, J = 7.4, 1H), 9.05 (t, J = 7.8, 1H), 6.52 (t, J = 7.7, 1H), 2.60 (d, J = 8.1, 1H), −2.23 (t, J = 7.7, 1H); $(Ph)_2PCH_2P(O)(Ph)_2$, −2.76 (m, 2H, CH_2), 18.10 (m, 2H), 10.22 (t, J = 7.5, 2H), 9.70 (t, J = 7.7, 2H), 8.16 (t, J = 7.4, 2H), 7.71 (m, 4H), 7.37 (t, J = 6.3, 2H), 7.21 (m, 4H), 7.13 (m, 2H).

[ReL¹(P(Ph)₂(CH₂)₂P(O)(Ph)₂)Cl₃]. Yield: 85% (Found: C, 50.65; H, 3.50; N, 3.18. Calc. for $C_{38}H_{32}N_2O_2P_2Cl_3Re$: C, 50.53; H, 3.57; N, 3.10%). UV-vis [λ_{max}/nm (ε/dm³ mol⁻¹ cm⁻¹), CH_2Cl_2 solution]: 678 (1790), 517 (920), 483^{sh} (1030), 444 (1350), 401 (2030), 316 (9710). IR(cm⁻¹): 309, 325 (Re–Cl), 1179 (P–O), 1604 (C=N). ^{1}H NMR [δ (J/Hz), $CDCl_3$ solution]: L¹, 18.84 (d, J = 6.6, 1H), 17.09 (d, J = 7.8, 1H), 15.17 (d, J = 6.1, 1H), 8.39 (t, J = 6.7, 1H), 7.12 (t, J = 6.8, 1H), 6.74 (t, J = 7.5, 1H), 0.52 (t, J = 7.6, 1H), −3.18 (d, J = 7.5, 1H); $(Ph)_2P(CH_2)_2P(O)(Ph)_2$, 6.39 (m, 2H, CH_2), 4.14 (m, 2H, CH_2), 16.58 (d, J = 6.9, 2H), 15.57 (d, J = 6.9, 2H), 9.39 (t, J = 7.4, 2H), 9.08 (t, J = 7.4, 2H), 8.65 (m, 2H), 7.48 (m, 2H), 6.66 (t, J = 6.3, 2H), 5.9–6.1 (m, 2H), 5.57 (t, J = 7.8, 2H), 5.45 (t, J = 8.6, 2H).

[ReL²(P(Ph)₂(CH₂)₂P(O)(Ph)₂)Cl₃]. Yield: 83% (Found: C, 49.60; H, 3.58; N, 3.01. Calc. for $C_{38}H_{32}N_2OP_2SCl_3Re$: C, 49.65; H, 3.51; N, 3.05%). UV-vis [λ_{max}/nm (ε/dm³ mol⁻¹ cm⁻¹), CH_2Cl_2 solution]: 701 (3360), 512 (1920), 460^{sh} (2720), 419 (3560), 324 (12970). IR(cm⁻¹): 308, 332 (Re–Cl), 1191 (P–O), 1604 (C=N). ^{1}H NMR [δ (J/Hz), $CDCl_3$ solution]: L², 18.57 (i, 1H), 17.82 (i, 1H), 12.56 (i, 1H), 9.50 (t, J = 7.5, 1H), 9.04 (t, J = 7.5, 1H), 6.53 (t, J = 7.5, 1H), 2.56 (d, J = 7.5, 1H), −2.30 (t, J = 7.7, 1H); $(Ph)_2P(CH_2)_2P(O)(Ph)_2$, −2.70 (m, 2H, CH_2), −3.71 (m, 2H, CH_2), 18.04 (m, 2H), 12.20 (t, J = 6.8, 2H), 9.68 (t, J = 7.4, 2H), 8.14 (t, J = 7.4, 2H), 7.78 (m, 4H), 7.40 (t, J = 8.0, 4H), 7.14 (i, 2H), 6.76 (d, J = 6.4, 2H).

[ReL¹(P(Ph)₂(CH₂)₃P(O)(Ph)₂)Cl₃]. Yield: 83% (Found: C, 51.19; H, 3.86; N, 3.00. Calc. for $C_{39}H_{34}N_2O_2P_2Cl_3Re$: C, 51.07; H, 3.74; N, 3.05%). UV-vis [λ_{max}/nm (ε/dm³ mol⁻¹ cm⁻¹), CH_2Cl_2 solution]: 675 (1690), 517 (1170), 482^{sh} (1440), 443 (1850), 415 (2180), 315 (14110). IR(cm⁻¹): 312, 327 (Re–Cl), 1160 (P–O), 1606 (C=N). ^{1}H NMR [δ (J/Hz), $CDCl_3$ solution]: L¹, 24.28 (d, J = 8.7, 1H), 17.62 (d, J = 8.1, 1H), 11.82 (d, J = 7.8, 1H), 11.54 (t, J = 7.7, 1H), 9.46 (t, J = 7.4, 1H), 9.11 (t, J = 7.4, 1H), 6.18 (d, J = 7.8, 1H), −0.26 (t, J = 7.7, 1H); $(Ph)_2P(CH_2)_3P(O)(Ph)_2$, 3.85 (m, 2H, CH_2), 3.05 (m, 2H, CH_2), 2.49 (m, 2H, CH_2), 19.58 (d, J = 6.1, 2H), 18.45 (d, J = 7.5, 2H), 16.49 (t, J = 6.5, 2H), 8.68 (t, J = 6.0, 2H), 8.59 (m, 2H), 8.16 (t, J = 7.7, 2H), 7.98 (d, J = 7.8, 2H), 7.83 (m, 2H), 7.69 (i, 2H), 7.52 (t, J = 6.5, 2H).

[ReL²(P(Ph)₂(CH₂)₃P(O)(Ph)₂)Cl₃]. Yield: 80% (Found: C, 50.29; H, 3.77; N, 3.08. Calc. for $C_{39}H_{34}N_2OP_2SCl_3Re$: C, 50.19; H, 3.67; N, 3.00%). UV-vis [λ_{max}/nm (ε/dm³ mol⁻¹ cm⁻¹), CH_2Cl_2 solution]: 692 (3010), 512 (2350), 460^{sh} (2970), 425 (3830), 329 (17560). IR(cm⁻¹): 325 (Re–Cl), 1195 (P–O), 1610 (C=N). ^{1}H NMR [δ (J/Hz), $CDCl_3$ solution]: L², 24.69 (d, J = 8.4, 1H), 17.86 (i, 1H), 17.37 (t, J = 6.6, 1H), 12.51 (d, J = 7.8, 1H), 9.60 (t, J = 7.7, 1H), 9.09 (t, J = 7.7, 1H), 6.42 (d, J = 8.2, 1H), −1.49 (t, J = 7.7, 1H); $(Ph)_2P(CH_2)_3P(O)(Ph)_2$, 4.11 (m, 2H, CH_2), 3.74 (m, 2H, CH_2), 2.77 (m, 2H, CH_2), 7.6–7.7 (m, 4H), 7.53 (d, J = 7.6, 2H), 7.49 (m, 4H), 7.35 (m, 4H), 7.12 (m, 4H), 6.81 (d, J = 7.7, 2H).

[ReL¹(P(Ph)₂(CH₂)₄P(O)(Ph)₂)Cl₃]. Yield: 80% (Found: C, 51.50; H, 3.98; N, 2.90. Calc. for $C_{40}H_{36}N_2O_2P_2Cl_3Re$: C, 51.59; H, 3.90; N, 3.01%). UV-vis [λ_{max}/nm (ε/dm³ mol⁻¹ cm⁻¹), CH_2Cl_2 solution]: 674 (1720), 517 (1180), 482^{sh} (1450), 442 (1890), 414 (2230), 315 (14710). IR(cm⁻¹): 310, 330 (Re–Cl), 1193 (P–O), 1607 (C=N). ^{1}H NMR [δ (J/Hz), $CDCl_3$ solution]: L¹, 24.25 (d, J = 7.8, 1H), 11.19 (t, J = 6.3, 1H), 10.76 (t, J = 7.7, 1H), 10.62 (t, J = 7.8, 1H), 9.71 (d, J = 7.8, 1H), 9.51 (d, J = 8.1, 1H), 7.07 (d, J = 8.7, 1H), −11.94 (t, J = 7.5, 1H); $(Ph)_2P(CH_2)_4P(O)(Ph)_2$, 6.75 (m, 2H, CH_2), 6.11 (m, 2H, CH_2), 5.22 (m, 2H, CH_2), 4.06 (m, 2H, CH_2), 19.53 (i, 2H), 18.39 (d, J = 7.5, 2H), 16.41 (t, J = 6.3, 2H), 10.55 (d, J = 7.8, 2H), 8.56 (m, 4H), 7.63 (d, J = 6.7, 4H), 7.41 (d, J = 6.0, 4H).

[ReL²(P(Ph)₂(CH₂)₄P(O)(Ph)₂)Cl₃]. Yield: 76% (Found: C, 50.78; H, 3.84; N, 2.90. Calc. for $C_{40}H_{36}N_2OP_2SCl_3Re$: C, 50.72; H, 3.83; N, 2.96%). UV-vis [λ_{max}/nm (ε/dm³ mol⁻¹ cm⁻¹), CH_2Cl_2 solution]: 688 (3200), 510 (1430), 461^{sh} (1940), 429 (2340), 329 (13650). IR(cm⁻¹): 307, 325 (Re–Cl), 1170 (P–O), 1605 (C=N). ^{1}H NMR [δ (J/Hz), $CDCl_3$ solution]: L², 24.70 (d, J = 8.1, 1H), 17.88 (i, 1H), 17.39 (t, J = 6.6, 1H), 12.52 (d, J = 7.5, 1H), 9.61 (t, J = 7.8, 1H), 9.11 (t, J = 7.7, 1H), 6.44 (d, J = 8.1, 1H), −1.47 (t, J = 7.8, 1H); $(Ph)_2P(CH_2)_4P(O)(Ph)_2$, 4.20 (m, 2H, CH_2), 2.32 (m, 2H, CH_2), 2.02 (m, 2H, CH_2), 0.86 (m, 2H, CH_2), 7.70 (t, J = 9.1, 4H), 7.47 (m, 6H), 7.36 (m, 2H), 7.0–7.2 (m, 4H), 6.7–6.8 (m, 4H).

[ReL(PMe$_y$Ph$_{3-y}$)Cl$_3$] 5. These were prepared by the reaction of [ReL(OPMe$_y$Ph$_{3-y}$)Cl$_3$] with excess PMe$_y$Ph$_{3-y}$ in boiling benzene. Details are given below for a representative case.

[ReL¹(PMe₂Ph)Cl₃]. To a solution of [ReL¹(OPMe$_2$Ph)Cl$_3$] (70 mg, 0.10 mmol) in 30 cm³ benzene was added PMe$_2$Ph (83 mg, 0.60 mmol), and the mixture was heated to reflux for 1 h. The resulting solution was evaporated to dryness and the residue was washed several times with hexane (to remove excess PMe$_2$Ph). The residue was dissolved in 5 cm³ dichloromethane and was subjected to chromatography on a silica gel column. A green band was eluted with a benzene–acetonitrile (25 : 10) mixture. Solvent removal from the eluate under reduced pressure afforded [ReL¹(PMe$_2$Ph)Cl$_3$] as a green solid which was dried under vacuum over fused $CaCl_2$. Yield: 88% (Found: C, 38.38; H, 3.00; N, 4.59. Calc. for $C_{20}H_{19}N_2OPCl_3Re$: C, 38.32; H, 3.05; N, 4.47%). UV-vis [λ_{max}/nm (ε/dm³ mol⁻¹ cm⁻¹), CH_2Cl_2 solution]: 691 (2340), 518 (1480), 483^{sh} (1720), 449 (2010), 385 (3160), 317 (14620). IR(cm⁻¹): 306, 326 (Re–Cl), 1600 (C=N). ^{1}H NMR [δ (J/Hz), $CDCl_3$ solution]: L¹, 20.73 (t, J = 6.5, 1H), 19.95 (d, J = 6.3, 1H), 19.10 (d, J = 8.1, 1H), 9.17 (t, J = 7.5, 1H), 6.28 (d, J = 9.6, 1H), 5.68 (t, J = 7.8, 1H); 0.86 (d, J = 7.5,1H), −3.02 (t, J = 7.8, 1H); PMe$_2$Ph, 3.94 (s, 3H, PCH$_3$), 3.14 (s, 3H, PCH$_3$), 17.62 (d, J = 7.2, 2H), 9.42 (t, J =7.7, 2H), 8.69 (t, J = 7.5, 1H).

[ReL²(PMe₂Ph)Cl₃]. Yield: 87% (Found: C, 37.49; H, 3.12; N, 4.30. Calc. for $C_{20}H_{19}N_2PSCl_3Re$: C, 37.36; H, 2.98; N, 4.36%). UV-vis [λ_{max}/nm (ε/dm³ mol⁻¹ cm⁻¹), CH_2Cl_2 solution]: 709 (3390), 529 (1670), 460^{sh} (2050), 413 (3470), 328 (14030). IR(cm⁻¹): 308, 327 (Re–Cl), 1600 (C=N). ^{1}H NMR [δ (J/Hz), $CDCl_3$ solution]: L², 15.87 (d, J = 6.9, 1H), 15.27 (t, J = 6.4, 1H), 9.20 (d, J = 7.8, 1H), 7.4–7.6 (m, 2H), 5.93 (t, J = 8.1, 1H), 2.72 (d, J = 7.2, 1H), −5.29 (t, J = 6.4, 1H); PMe$_2$Ph, 7.81 (s, 3H, PCH$_3$), 7.17 (s, 3H, PCH$_3$), 8.5–8.8 (m, 3H), 8.24 (t, J = 7.6, 2H).

[ReL¹(PMePh₂)Cl₃]. Yield: 83% (Found: C, 43.50; H, 3.00; N, 4.17. Calc. for $C_{25}H_{21}N_2OPCl_3Re$: C, 43.58; H, 3.07; N, 4.07%). UV-vis [λ_{max}/nm (ε/dm³ mol⁻¹ cm⁻¹), CH_2Cl_2 solution]: 686 (1780), 514 (870), 483^{sh} (940), 447 (1090), 387 (1540), 322 (8450). IR(cm⁻¹): 309, 327 (Re–Cl), 1600 (C=N). ^{1}H NMR [δ (J/Hz), $CDCl_3$ solution]: L¹, 20.18 (t, J = 7.1, 1H), 18.52 (d, J = 8.1, 1H), 17.51 (d, J = 6.3, 1H), 9.11 (t, J = 7.5, 1H), 6.27 (d, J = 7.8, 1H), 5.67 (t, J = 7.8, 1H), 1.41 (d, J = 7.8, 1H), −3.31 (t, J = 7.8, 1H); PMePh$_2$, 3.08 (s, 3H, PCH$_3$), 15.83 (d, J = 7.2, 2H), 14.87 (d, J = 6.9, 2H), 9.30 (t, J = 7.2, 2H), 8.99 (t, J = 7.8, 1H), 8.81 (t, J = 7.7, 1H), 8.59 (t, J = 7.6, 2H).

[ReL²(PMePh₂)Cl₃]. Yield: 86% (Found: C, 42.68; H, 3.09; N, 3.90. Calc. for $C_{25}H_{21}N_2PSCl_3Re$: C, 42.59; H, 3.00; N, 3.97%). UV-vis [λ_{max}/nm (ε/dm³ mol⁻¹ cm⁻¹), CH_2Cl_2 solution]: 705 (3480), 524 (1920), 463^{sh} (2060), 414 (3580), 326 (14450).

IR(cm^{-1}): 310, 330 (Re–Cl), 1604 (C=N). ^{1}H NMR [δ (*J*/Hz), $CDCl_3$ solution]: L^2, 20.17 (t, *J* = 6.6, 1H), 18.51 (d, *J* = 8.4, 1H), 17.47 (d, *J* = 6.3, 1H), 8.99 (t, *J* = 8.0, 1H), 6.27 (d, *J* = 8.4, 1H), 5.57 (t, *J* = 8.1, 1H), 2.00 (d, *J* = 6.3, 1H), −3.31 (t, *J* = 7.8, 1H); $PMePh_2$, 3.07 (s, 3H, PCH_3), 12.83 (d, *J* = 7.2, 2H), 11.88 (d, *J* = 7.5, 2H), 9.31 (t, *J* = 7.6, 2H), 9.11 (t, *J* = 7.6, 2H), 8.51 (t, *J* = 7.4, 1H), 8.29 (t, *J* = 7.4, 1H).

[ReL^1(PPh$_3$)Cl$_3$]. Yield: 86% (Found: C, 47.90; H, 3.15; N, 3.85. Calc. for $C_{30}H_{23}N_2OPCl_3Re$: C, 47.98; H, 3.09; N, 3.73%). UV-vis [λ_{max}/nm (ε/dm^3 mol^{-1} cm^{-1}), CH_2Cl_2 solution]: 685 (1930), 514 (980), 483^{sh} (1060), 449 (1280), 399 (1920), 318 (9520). IR(cm^{-1}): 310, 325 (Re–Cl), 1600 (C=N). ^{1}H NMR [δ (*J*/Hz), $CDCl_3$ solution]: L^1, 19.82 (t, *J* = 6.6, 1H), 18.19 (d, *J* = 8.4, 1H), 15.98 (d, *J* = 6.3, 1H), 8.75 (t, *J* = 7.4, 1H), 6.12 (d, *J* = 8.7, 1H), 5.49 (t, *J* = 7.8, 1H), 0.94 (d, *J* = 7.8, 1H), −3.81 (t, *J* = 8.1, 1H); PPh_3, 13.32 (d, *J* = 6.6, 6H), 8.80 (t, *J* = 7.3, 6H), 8.42 (t, *J* = 7.5, 3H).

[ReL^2(PPh$_3$)Cl$_3$]. Yield: 85% (Found: C, 46.90; H, 2.98; N, 3.60. Calc. for $C_{30}H_{23}N_2PSCl_3Re$: C, 46.97; H, 3.02; N, 3.65%). UV-vis [λ_{max}/nm (ε/dm^3 mol^{-1} cm^{-1}), CH_2Cl_2 solution]: 707 (3260), 526 (1910), 463^{sh} (2170), 413 (3320), 326 (11610),. IR(cm^{-1}): 310, 325 (Re–Cl), 1600 (C=N). ^{1}H NMR [δ (*J*/Hz), $CDCl_3$ solution]: L^2, 18.85 (t, *J* = 6.3, 1H), 17.71 (d, *J* = 7.9, 1H), 11.54 (d, *J* = 5.2, 1H), 8.87 (t, *J* = 7.7, 1H), 8.03 (d, *J* = 7.7, 1H), 6.53 (t, *J* = 7.9, 1H), 2.02 (d, *J* = 7.7, 1H), −2.05 (t, *J* = 7.5, 1H); PPh_3, 13.06 (d, *J* = 6.7, 6H), 8.76 (t, *J* = 7.3, 6H), 8.43 (t, *J* = 7.3, 3H).

[ReL(OP(Ph)$_2$CH$_2$P(Ph)$_2$)Cl$_3$]NO$_3$ 2$^+$NO$_3^-$. The two compounds (L = L^1, L^2) were prepared by the same general procedure. The details for L = L^1 are given below.

[ReL^1(OP(Ph)$_2$CH$_2$P(Ph)$_2$)Cl$_3$]NO$_3$. To a solution of [$ReL^1(OP(Ph)_2CH_2P(Ph)_2)Cl_3$] (75 mg, 0.08 mmol) in 15 cm^3 acetonitrile was added dilute aqueous HNO_3 (0.1 M, 3 cm^3) and the solution was stirred at room temperature for 0.25 h. During this time the solution color changed from violet to orange. Solvent removal under reduced pressure afforded [$ReL^1(OP(Ph)_2CH_2P(Ph)_2)Cl_3]NO_3$ as an orange solid. The solid was washed thoroughly with water to remove the adherent nitric acid and then dried under vacuum over fused $CaCl_2$. Yield: 61% (Found: C, 46.60; H, 3.27; N, 4.33. Calc. for $C_{37}H_{30}N_3O_5P_2Cl_3Re$: C, 46.72; H, 3.18; N, 4.42%). UV-vis [λ_{max}/nm (ε/dm^3 mol^{-1} cm^{-1}), CH_2Cl_2 solution]: 443^{sh} (800), 361^{sh} (2760), 324 (13090), 311 (14090). IR(cm^{-1}): 325, 337 (Re–Cl), 1115 (O–P), 1611 (C=N), 1384 (N–O, NO_3^-). ^{1}H NMR [δ, $CDCl_3$ solution]: L^1, 54.22 (1H), 16.96 (1H), 15.86 (1H), 11.57 (1H), 10.14 (1H), 7.60 (1H), 6.34 (1H), 4.17 (1H); $Ph_2PCH_2PPh_2$, 8.49 (4H), 7.95 (4H), 7.74 (4H), 7.50 (4H), 6.88 (4H), 6.12 (2H).

[ReL^2(OP(Ph)$_2$CH$_2$P(Ph)$_2$)Cl$_3$]NO$_3$. Yield: 60% (Found: C, 45.99; H, 3.19; N, 4.20. Calc. for $C_{37}H_{30}N_3O_4P_2SCl_3Re$: C, 45.95; H, 3.13; N, 4.34%). UV-vis [λ_{max}/nm (ε/dm^3 mol^{-1} cm^{-1}), CH_2Cl_2 solution]: 433^{sh} (1340), 386^{sh} (3080), 316 (8100), 296 (8380). IR(cm^{-1}): 325, 338 (Re–Cl), 1118 (O–P), 1613 (C=N), 1384 (N–O, NO_3^-). ^{1}H NMR [δ, $CDCl_3$ solution]: L^2, 54.67 (1H), 18.84 (1H), 16.09 (1H), 15.03 (1H), 11.55 (1H), 10.21 (1H), 4.15 (1H), 2.52 (1H); $Ph_2PCH_2PPh_2$, 8.34 (2H), 7.82 (4H), 7.65 (4H), 7.51 (4H), 7.39 (4H), 6.56(2H), 4.83 (2H).

[ReL(OPPh$_3$)Cl$_3$]NO$_3$ 3$^+$NO$_3^-$. The same procedure used for **2**$^+$$NO_3^-$ was employed for **3**$^+$$NO_3^-$ as well.

[ReL^1(OPPh$_3$)Cl$_3$]NO$_3$. Yield: 66% (Found: C, 43.40; H, 2.88; N, 5.01. Calc. for $C_{30}H_{23}N_3O_5PCl_3Re$: C, 43.46; H, 2.80; N, 5.07%). UV-vis [λ_{max}/nm (ε/dm^3 mol^{-1} cm^{-1}), CH_2Cl_2 solution]: 442^{sh} (820), 361^{sh} (2590), 323 (11690), 312 (12580). IR(cm^{-1}): 328, 340 (Re–Cl), 1117 (O–P), 1610 (C=N), 1384 (N–O, NO_3^-). ^{1}H NMR [δ, $CDCl_3$ solution]: L^1, 56.80 (1H), 34.54 (1H), 17.81 (1H), 12.88 (1H), 11.64 (1H), 10.07 (1H), 7.61 (1H), 5.67 (1H); PPh_3, 9.86 (6H), 7.74 (3H), 6.75 (6H).

[ReL^2(OPPh$_3$)Cl$_3$]NO$_3$. Yield: 64% (Found: C, 42.70; H, 2.70; N, 4.83. Calc. for $C_{30}H_{23}N_3O_4PSCl_3Re$: C, 42.64; H, 2.74; N, 4.97%). UV-vis [λ_{max}/nm (ε/dm^3 mol^{-1} cm^{-1}), CH_2Cl_2 solution]: 434^{sh} (1390), 385^{sh} (3300), 319 (8840), 297 (8850). IR(cm^{-1}): 326, 339 (Re–Cl), 1118 (O–P), 1613 (C=N), 1384 (N–O, NO_3^-). ^{1}H NMR [δ, $CDCl_3$ solution]: L^2, 55.35 (1H), 33.09 (1H), 16.37 (1H), 11.44 (1H), 10.20 (1H), 8.63 (1H), 6.19 (1H), 4.23 (1H); PPh_3, 8.41 (6H), 6.31 (3H), 5.23 (6H).

Rate measurements

The rate of the single oxygen atom transfer reaction of eqn. (2) was determined spectrophotometrically (quartz cell, path length 1 cm) in the case of $Ph_2P(CH_2)_4PPh_2$. A known excess of the diphosphine was added to a solution of [$ReL^1(O)Cl_3$] (1.25×10^{-4} M) in dichloromethane at 308 K and the absorbance A_t monitored for the peak at 737 nm as a function of time (*t*). The time dependent spectra are characterised by isosbestic points at 425 and 491 nm. The absorbance A_α at 737 nm at the end of the reaction (6 h) was also monitored. The calculations were performed using Microcal Origin V 2.8 (E. Northampton, Microcal Origin Inc., 1991) and GraFit, Data Analysis & Graphics Program, V 3.00 (R. J. Leatherbarrow, Erithacus Software Ltd., 1992). The observed rate constants k_{obs} were determined from the slope of the highly linear plot (correlation constant 0.990–0.996) of $\ln(A_\alpha - A_t)$ *versus t*. The rate constant *k* was obtained from the linear plot (correlation constant 0.9999) of k_{obs} *versus* concentration of the diphosphine. The rate constant for the reaction of [$ReL^2(O)Cl_3$] with the diphosphine was similarly determined.

The rate of the twin isomerization process of eqn. (4) was also followed spectrophotometrically at 308 K. Time dependent absorbances A_t were measured at 579 nm and 585 nm for the L^1 and L^2 complexes respectively and A_α values were obtained at the end of the reaction (1 to 7 days depending on L and *x*). Rate constants were determined from the linear plots (correlation constants 0.996–0.999) of $-\ln(A_t - A_\alpha)$ *versus t*. Variable concentration ($1-4 \times 10^{-4}$ M) studies carried out in the cases of *x* = 1 revealed that the rate constants were independent of concentration consistent with first order kinetics. The plot of rate constants against diphosphine spacer length (*x*) follows a single exponential decay pattern (Fig. 7) with reduced χ^2 values of $\approx 10^{-8}$ and $\approx 10^{-9}$ for L^1 and L^2 complexes respectively.

Crystallography

Single crystals of the complexes **3a**, **3b**$^+$$NO_3^-$·0.5$CH_2Cl_2$, **5a** and **5b**·$H_2O$ were grown by slow diffusion of hexane into dichloromethane solutions of the respective compounds. During synthesis all the vacuum dried complexes occur in a non-solvated form, *vide supra*. Single crystal formation however requires solvation in two of the four cases examined here. Data were collected on a Nicolet R3m/V four circle diffractometer with graphite monochromated Mo-K_α radiation (λ = 0.71073 Å) by the ω-scan technique in the range $3 \le 2\theta \le 50°$ for compounds **3a**, **3b**$^+$$NO_3^-$·0.5$CH_2Cl_2$ and **5b**·H_2O and in the range $3 \le 2\theta \le 47°$ for compound **5a**. In all the cases the data were corrected for Lorentz-polarization and absorption.[18] The metal atoms were located from Patterson maps and the rest of the non-hydrogen atoms emerged from successive Fourier synthesis. The structures were refined by full-matrix least-squares procedures on F^2. The non-hydrogen atoms were refined anisotropically and the hydrogen atoms (excepting those in solvents of crystallisation) were included in calculated positions. The dichloromethane molecule in **3b**$^+$$NO_3^-$·0.5$CH_2Cl_2$ is highly disordered and could be only roughly modelled (four-fold disorder around one chlorine atom acting as a pivot). Calculations were performed using the SHELXTL™ V 5.03[19] program package. Significant crystal data are listed in Table 6.

CCDC reference numbers 214947–214950.

See http://www.rsc.org/suppdata/dt/b3/b307834e/ for crystallographic data in CIF or other electronic format.

Table 6 Crystal data for complexes **3a**, **3b**$^{+}NO_3^{-}\cdot 0.5CH_2Cl_2$, **5a** and **5b**$\cdot H_2O$

Complex	**3a**	**3b**$^{+}NO_3^{-}\cdot 0.5CH_2Cl_2$	**5a**	**5b**$\cdot H_2O$
Formula	$C_{20}H_{19}N_2OPSCl_3Re$	$C_{30.5}H_{24}N_3O_4PSCl_4Re$	$C_{20}H_{19}N_2OPCl_3Re$	$C_{25}H_{23}N_2O_2PCl_3Re$
M	658.95	887.56	626.89	706.97
System	Monoclinic	Triclinic	Monoclinic	Monoclinic
Space group	$P2_1$	$P\bar{1}$	$P2_1/c$	$C2/c$
a/Å	10.597(2)	13.989(3)	9.266(5)	18.008(4)
b/Å	8.445(2)	14.769(3)	14.394(4)	8.481(2)
c/Å	12.674(3)	16.881(3)	16.311(5)	34.252(7)
α/°	90	86.26(3)	90	90
β/°	96.20(3)	88.95(3)	101.40(3)	94.65(3)
γ/°	90	75.15(3)	90	90
U/Å^3	1127.6(4)	3364.1(12)	2132.6(14)	5214(2)
Z	2	4	4	8
D/mg m^{-3}	1.941	1.752	1.953	1.801
T/K	293	293	293	293
μ/mm^{-1}	5.922	4.079	6.163	5.056
Unique reflections	2095	10539	3149	4580
R_1, $wR_2[I>2\sigma(I)]$	0.0281, 0.0694	0.0595, 0.1482	0.0405, 0.0920	0.0391, 0.1053
All data	0.0290, 0.0707	0.0739, 0.1710	0.0641, 0.1189	0.0461, 0.1263

Acknowledgements

We thank the Department of Science and Technology, and Council of Scientific and Industrial Research, New Delhi for financial support. We are thankful to Prof. G. K. Lahiri and Dr S. Chattopadhyay for help.

References

1 B. K. Dirghangi, M. Menon, A. Pramanik and A. Chakravorty, *Inorg. Chem.*, 1997, **36**, 1095.
2 I. Chakraborty, S. Bhattacharyya, S. Banerjee, B. K. Dirghangi and A. Chakravorty, *J. Chem. Soc., Dalton Trans.*, 1999, 3747.
3 S. Banerjee, S. Bhattacharyya, B. K. Dirghangi, M. Menon and A. Chakravorty, *Inorg. Chem.*, 2000, **39**, 6.
4 S. B. Seymore and S. N. Brown, *Inorg. Chem.*, 2000, **39**, 325.
5 R. Conry and J. M. Mayer, *Inorg. Chem.*, 1990, **29**, 4862.
6 G. Battistuzzi, M. Barsari and R. Battistuzzi, *Polyhedron*, 1997, **16**, 2093.
7 J. F. Rowbottom and G. Wilkinson, *J. Chem. Soc., Dalton Trans.*, 1972, 826.
8 S. Bhattacharyya, I. Chakraborty, B. K. Dirghangi and A. Chakravorty, *Inorg. Chem.*, 2001, **40**, 286.
9 S. Bhattacharyya, I. Chakraborty, B. K. Dirghangi and A. Chakravorty, *Chem. Commun.*, 2000, 1813.
10 X. L. R. Fontaine, E. H. Fowles, T. P. Layzell, B. L. Shaw and M. J. Thornton-Pett, *J. Chem. Soc., Dalton Trans.*, 1991, 1519.
11 J. Gangopadhyay, S. Sengupta, S. Bhattacharyya, I. Chakraborty and A. Chakravorty, *Inorg. Chem.*, 2002, **41**, 2616.
12 K. Nakamoto, *Infrared and Raman Spectra of Inorganic and Coordination Compounds, Theory and Applications in Inorganic Chemistry*, Part A, John Wiley and Sons, Inc., New York, 5th edn., 1997, p. 182.
13 S. Bhattacharyya, S. Banerjee, B. K. Dirghangi, M. Menon and A. Chakravorty, *J. Chem. Soc., Dalton Trans.*, 1999, 155.
14 F. Tisato, F. Refosco, C. Bolzati, A. Cagnolini, S. Gatto and G. Bandoli, *J. Chem. Soc., Dalton Trans.*, 1997, 1421.
15 P. J. Flory, *Principles of Polymer Chemistry*, Cornell University Press, Ithaca and London, 4th edn., 1990, p. 399.
16 P. Ghosh, A. Pramanik, N. Bag and A. Chakravorty, *J. Chem. Soc., Dalton Trans.*, 1992, 1883.
17 N. Serpone and S. P. Sengupta, *Cryst. Struct. Commun.*, 1980, **9**, 965.
18 A. C. T. North, D. C. Philips and F. S. Mathews, *Acta Crystallogr., Sect. A*, 1968, **24**, 351.
19 G. M. Sheldrick, SHELXTL V 5.03, Bruker Analytical X-ray Systems, Madison, WI, 1994.